Surfaces

DOI: 10.1002/ange.200600367

Adhesion of a Free-Standing Newton Black Film onto a Solid Substrate**

Jean-Jacques Benattar, Michael Nedyalkov, Fuk Kay Lee, and Ophelia K. C. Tsui*

Newton black films (NBFs) are self-assembled molecular bilayers of surfactant that usually contain a residual hydration layer in the core upon maximal drainage.[1–10] Because the films are so thin, optical light reflected from the interfaces interferes destructively, thereby giving NBFs a black appearance and hence their name.

We recently reported a process for the insertion of protein molecules into an NBF by controlling the chemical potential of the protein molecules in the solution from which the NBF is extracted and self-assembled.[11–13] Such a process has been shown to allow the formation of a dense monolayer of protein molecules, which can be water soluble (for example, bovine serum albumin) or insoluble (for example, the outer membrane protein OmpA), inside the NBF bilayer. Since the driving force is independent of the nature of the objects being inserted, sufficiently small molecules or nanoparticles that can be made soluble in water by an appropriate surfactant would be suitable candidates for this process. It may thus provide a powerful method for making 2D assemblies of a large variety of molecules and nanoparticles, thereby opening up new opportunities for fundamental research and new technologies.[14–16]

NBFs have only been made in the fragile free-standing form to date. To make such films amenable to practical applications, it is therefore necessary to find ways of depositing them onto a solid substrate. Herein, we show for the first time the transfer of an NBF to a solid substrate by bringing the substrate into contact with a "black bubble". A very large area (a few square centimeters) of the film can be transferred. The bubble is made from an aqueous solution of surfactant (hexaethylene glycol monododecyl ether ($C_{12}E_6$)) and the substrate is hydrophobized silicon. Results from X-ray reflectivity (XR) and atomic force microscopy (AFM) studies show a high degree of molecular organization in the deposited film.

The apparatus is shown in Figure 1. The main components are an air-tight glass chamber and a porous plate that is used to control the bubble drainage, which limits the top level of the solution. A conduit at the bottom connects the chamber to a reservoir containing the surfactant solution. A hole drilled in the center of the porous plate is connected to a gas pipe. The solution from the reservoir is allowed to fill the chamber, flushing the top of the porous plate. The substrate is mounted face-down on a vertical translation stage at the top of the chamber. An air bubble is formed on the porous plate by slowly injecting air through the pipe. Water is allowed to drain from the bubble until the top of the bubble appears black. The substrate is then steadily lowered towards the bubble, until the bubble film adheres to the substrate.

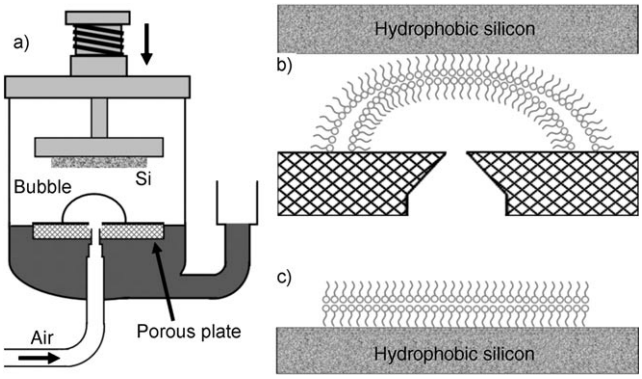

Figure 1. Schematic drawings illustrating the transfer of an NBF film from a "black bubble" (note that the film and the porous plate are not drawn at the same scale). a) A bubble is formed on the porous plate inside the chamber. b) When the top of the bubble film turns black, the silicon substrate is lowered to make contact with the bubble. c) A black film is transferred onto the silicon substrate.

Figure 2a shows the XR curve of a free-standing $C_{12}E_6$ NBF. It exhibits three distinct interference fringes. We fitted the curve by using the optical matrix formalism,[17] which assumes that the film is composed of a succession of slabs, and obtained the roughness at each interface, along with the thickness and electron density profile along the film normal. By assuming the $C_{12}E_6$ film to be a symmetric trilayer consisting of a central layer sandwiched between two identical external layers, the thickness of the film was deduced to be 60 Å, consistent with the value previously found for NBFs of this surfactant[7,11] and with the thickness reported for its monolayer.[18] The interfacial roughness is approximately 3 Å, which shows that the film is well ordered and homogeneous. The results are summarized in Table 1.

Figure 2b shows the XR curve of a similarly prepared $C_{12}E_6$ film transferred onto a silicon substrate. Two interference fringes with reduced definition are found. The fitted values of the film thickness and interfacial roughness are 48 and 7 Å, respectively. The fitting parameters are summarized

[*] Dr. J.-J. Benattar, Dr. M. Nedyalkov,[+] Dr. F. K. Lee
Service de Physique de l'Etat Condensé (CNRS URA 2464)
DSM/DRECAM/SPEC, CEA Saclay
91191 Gif sur Yvette Cedex (France)
Fax: (+33) 169-088-786
E-mail: Jean-Jacques.Benattar@cea.fr
Dr. O. K. C. Tsui
Department of Physics
Hong Kong University of Science and Technology
Clear Water Bay, Hong Kong (China)
[+] Permanent address:
Department of Physical Chemistry
University of Sofia
Blvd. James Bourchier 1, 1126 Sofia (Bulgaria)

[**] We thank Prof. Ichinose and Dr. Jin of the NIMS (Japan) for fruitful discussions on the formation of black films. We also acknowledge financial support from the France/Hong Kong Joint Research Scheme F-HK20/03T.

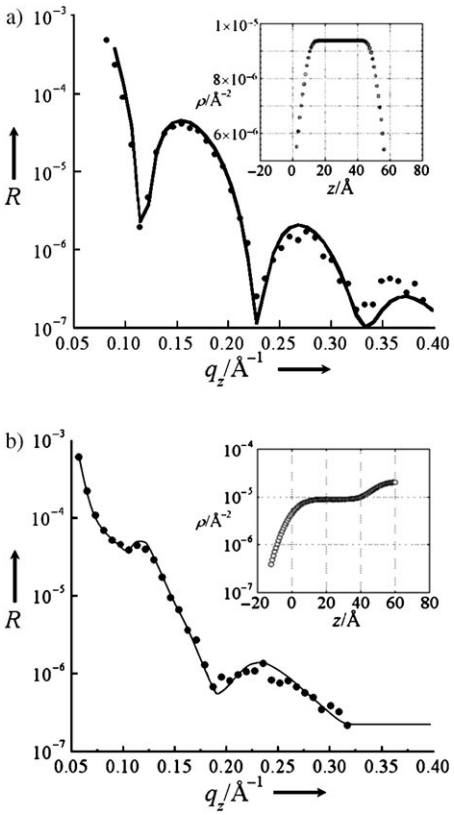

Figure 2. Plot of the reflectivity R as a function of the normal wave vector q_z for a) a free-standing $C_{12}E_6$ film and b) a transferred film. Solid circles are experimental data. The solid line in (a) is a model fit to the XR data, as detailed in the text. The solid line in (b) is a guide for the eye. The insets are profiles of the electron density along the film normals, deduced from fits of the corresponding XR data.

Table 1: Results of the fit to the XR data for a free-standing $C_{12}E_6$ film based on the model discussed in the text.

Layer	Thickness [Å]	δ[a]	Roughness [Å]
External	7.94	2.50×10^{-6}	3
Core	44.06	3.55×10^{-6}	3

[a] δ is the real part of the refractive index. $\delta=\lambda^2 r_e\rho/2\pi$, where $\lambda=$ 1.5405 Å is the X-ray wavelength, r_e is the classical electron radius, and ρ is the mean electron density.

in Table 2. The thickness of the deposited film is reduced by 12 Å and the interfacial roughness is increased by 3–4 Å compared with the free-standing film, which suggests that there is a morphological change caused by the transfer.

The thickness obtained by XR is an average value over the footprint of the incident X-ray, therefore the reduction of the total thickness, as well as the increase in the interfacial roughness suggest that there could be a small unevenness in

Table 2: Fitting parameters of the XR curve for a film of $C_{12}E_6$ deposited on a silicon substrate.

Layer	Thickness [Å]	δ	Roughness [Å]
Film	48	3.40×10^{-6}	7
Bulk Si	–	7.82×10^{-6}	6

the deposition, which may also explain the reduced contrast found in the interference fringes. It is possible that some local parts of the bilayer are torn off during the transfer. Another possibility is that the alkyl chains become tilted from the surface normal.[18] The quality of the film transfer is expected to improve with further experiments.

The XR measurements can only provide information about the structure along the film normal. AFM, however, can give complementary information about the in-plane structure of the film surface and the details of any local inhomogeneity. Figure 3 shows AFM topographic images of

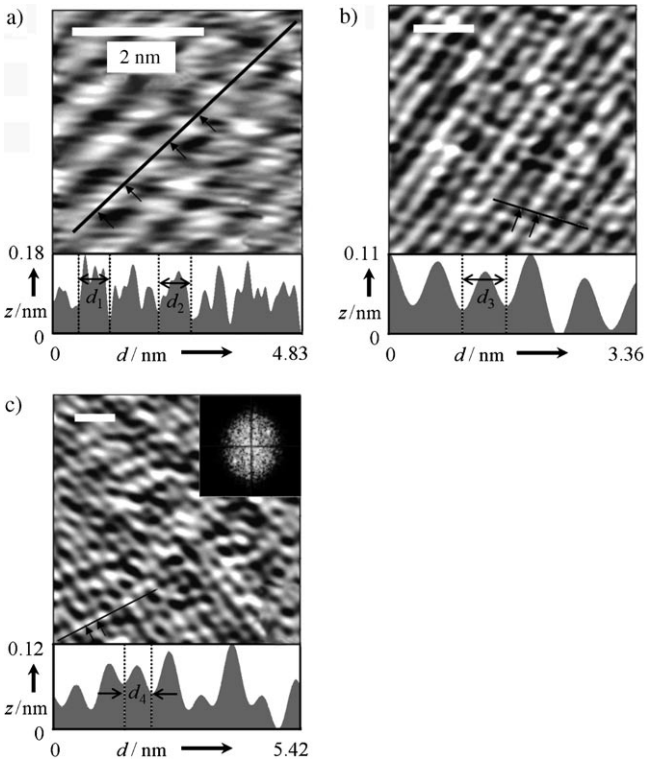

Figure 3. AFM topographic images of the transferred $C_{12}E_6$ films with different scan sizes of a) 4×4, b) 8×8, and c) 12×12 nm^2. The cross-sectional profile along an arbitrarily line drawn across the image is shown beneath each image. The distances d_1, d_2, d_3, and d_4 (bounded by arrows in images) are 0.60, 0.62, 0.61, and 0.60 nm, respectively. All scale bars represent 2 nm. The inset of (c) is the 2D Fourier transform of the real image in the main panel. High-frequency noise in the images was removed by Fourier filtering.

transferred $C_{12}E_6$ films with different scan sizes of a) 4×4, b) 8×8, and c) 12×12 nm^2 along different scan directions. Despite the different scan conditions employed for the imaging, all three images consistently show a chain structure with a periodicity of approximately 0.6 nm, close to the shortest distance between nearest-neighbor molecules.[19] The 2D Fourier transform shown in the inset of Figure 3c reveals a rather long correlation length for the surfactant molecules. The AFM topographic image of the same film over a much larger area of 2 μm^2 is shown in Figure 4, in which the surface can be seen to be quite homogeneous without noticeable aggregations. Hence, we deduce that the reduction of the total film thickness by 12 Å arises from a tilting of the surfactant

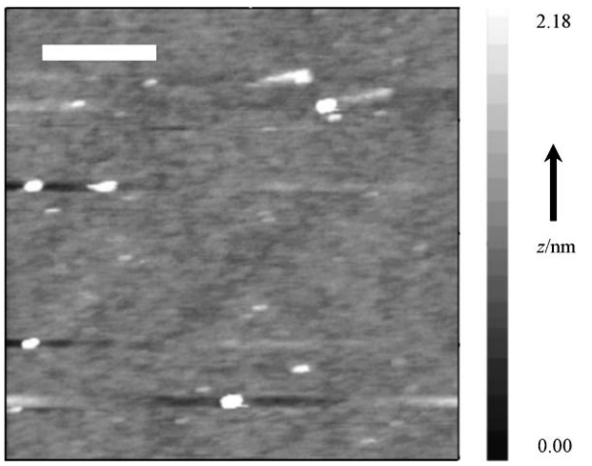

Figure 4. AFM image of a $C_{12}E_6$ film deposited on a silicon substrate, which shows that the film is continuous and smooth. A height (z) scale is to the right of the image. The white scale bar represents 500 nm. The bright spots are probably particulates from the air.

molecules after the transfer. In addition, no distortion is found in the image from a second scan of the same area, thus, showing that the transferred bilayer film is strongly adhered to the hydrophobic silicon substrate.

Free-standing black films have been studied for centuries, but with only a limited variety of techniques. In this study, we have succeeded for the first time in transferring a free-standing NBF onto a solid substrate, thereby allowing simultaneous characterization by XR and AFM. The data show that the molecular ordering of the black film is essentially preserved. This method may thus allow a more complete picture of an NBF's molecular structure to be determined. However, it is still in the early stages of development, and work is in progress to optimize the transfer process. In future studies, we will apply the insertion process to make an NBF with a variety of entities, including protein molecules, silver nanoparticles, and carbon nanotubes, in the core before transfer. The incorporation of nanoparticles or nanotubes is expected to lead to applications in electromechanical[15] or optoelectronic[20] devices, respectively.

Experimental Section

Materials: The nonionic surfactant hexaethylene glycol monododecyl ether ($C_{12}E_6$) was purchased from Sigma (Steinheim, Germany), and was used without further purification. NBFs of $C_{12}E_6$ were chosen for this study, because they have been extensively studied.[7,11] Furthermore, large and stable NBFs of $C_{12}E_6$ can usually be formed at a concentration higher than 0.5 mg mL^{-1}, which is approximately 15 times the critical micelle concentration. All solutions were prepared in ultrapure water (18.2 MΩ, milli-Q system), sonicated, and then filtered. The temperature was maintained at 23 ± 1 °C. Two-inch-diameter n-type Si (111) wafers (5–15 Ωcm) were used. They were first cleaned in a mixture of concentrated sulfuric acid and 33% hydrogen peroxide solution (3:1 ratio) at 120 °C for 10 min to remove any organic contaminants. The wafers were then treated to make the surface hydrophobic by putting them in 40% NH_4F for 20 min. They were then rinsed with ultrapure water and dried in argon gas for 30 min. This treatment produces atomically flat Si (111) surfaces with silicon monohydride terminations oriented normal to the surface.[21,22]

Characterization: XR experiments were carried out with a high-resolution reflectometer (Nonius OptiX) and a copper tube as an X-ray source ($\lambda = 1.5405$ Å). The free-standing films were drawn vertically by lifting a metallic frame at a slow constant rate inside an air-tight chamber in order to maintain a saturated vapor atmosphere. We measured the ratio $R(\theta) = I(\theta)/I_o$ at different incident angles θ, where I_o is the intensity of the incident X-ray beam and $I(\theta)$ is the intensity of the beam reflected off the film. From the specular reflectivity, we could deduce the interfacial roughness, the film thickness, and the electron density profile. The in-plane structure of the surfactant film was investigated by AFM topographic imaging with a Seiko Instruments (Chiban, Japan) SPA300HV model equipped with a platinum-coated silicon integrated cantilever tip with a spring constant of 0.03–0.08 N m^{-1} and a tip radius of less than 32 nm (manufacturing specification). During imaging, the AFM was operated in the contact force mode with an applied normal force of approximately 50 pN.

Received: January 27, 2006
Revised: March 13, 2006
Published online: May 23, 2006

Keywords: black films · deposition · film transfer · surfactants · thin films

[1] O. Belorgey, J. J. Benattar, *Phys. Rev. Lett.* **1991**, *66*, 313.
[2] D. Exerowa, P. M. Kruglyakov, *Foam and Foam Films: Theory, Experiment, Application*, Elsevier, Amsterdam, **1998**.
[3] D. Sentenac, J. J. Benattar, *Phys. Rev. Lett.* **1998**, *81*, 160.
[4] F. Millet, J. J. Benattar, P. Perrin, *Phys. Rev. E* **1999**, *60*, 2045.
[5] F. Millet, J. J. Benattar, P. Perrin, *Macromolecules* **2001**, *34*, 7076.
[6] N. Cuvillier, F. Millet, V. Petkova, M. Nedyalkov, J. J. Benattar, *Langmuir* **2000**, *16*, 5029.
[7] J. J. Benattar, Q. Shen, S. Bratskaya, V. Petkova, M. P. Krafft, B. Pucci, *Langmuir* **2004**, *20*, 1047.
[8] V. Petkova, C. Sultanem, M. Nedyalkov, J. J. Benattar, M. E. Leser, C. Schmitt, *Langmuir* **2003**, *19*, 6942.
[9] C. Sultanem, S. Moutard, J. J. Benattar, F. Djedaïni-Pilard, B. Perly, *Langmuir* **2004**, *20*, 3311.
[10] J. Jin, J. Huang, I. Ichinose, *Angew. Chem.* **2005**, *117*, 4608; *Angew. Chem. Int. Ed.* **2005**, *44*, 4532.
[11] J. J. Benattar, M. Nedyalkov, J. Prost, A. Tiss, R. Verger, C. Guilbert, *Phys. Rev. Lett.* **1999**, *82*, 5297.
[12] V. Petkova, J. J. Benattar, M. Nedyalkov, *Biophys. J.* **2002**, *82*, 541.
[13] V. Petkova, J.-J. Benattar, M. Zoonens, J.-L. Popot, A. Polidori, S. Jasseron, B. Pucci, *Langmuir* **2006**, submitted.
[14] Y. Cui, Q. Wei, H. Park, C. M. Lieber, *Science* **2001**, *293*, 1289.
[15] R. H. Baughman, C. Cui, A. A. Zakhidov, Z. Iqbal, J. N. Barisci, G. M. Spinks, G. G. Wallace, A. Mazzoldi, D. De Rossi, A. G. Rinzler, O. Jaschinski, S. Roth, M. Kertesz, *Science* **1999**, *284*, 1340.
[16] Z. Zhong, D. Wang, Y. Cui, M. W. Bockrath, C. M. Lieber, *Science* **2003**, *302*, 1377.
[17] M. Born, E. Wolf, *Principles of Optics*, Pergamon, London, **1984**, pp. 51–60.
[18] J. R. Lu, Z. X. Li, R. K. Thomas, E. J. Staples, I. Tucker, J. Penfold, *J. Phys. Chem.* **1993**, *97*, 8012.
[19] D. C. McDermott, J. R. Lu, E. M. Lee, R. K. Thomas, A. R. Rennie, *Langmuir* **1992**, *8*, 1204.
[20] P. V. Kamat, *J. Phys. Chem. B* **2002**, *106*, 7729.
[21] G. S. Higashi, Y. J. Chabal, G. W. Trucks, K. Raghavachari, *Appl. Phys. Lett.* **1990**, *56*, 656.
[22] G. S. Higashi, R. S. Becker, Y. J. Chabal, A. J. Becker, *Appl. Phys. Lett.* **1991**, *58*, 1656.

